



저작자표시-비영리-변경금지 2.0 대한민국

이용자는 아래의 조건을 따르는 경우에 한하여 자유롭게

- 이 저작물을 복제, 배포, 전송, 전시, 공연 및 방송할 수 있습니다.

다음과 같은 조건을 따라야 합니다:



저작자표시. 귀하는 원저작자를 표시하여야 합니다.



비영리. 귀하는 이 저작물을 영리 목적으로 이용할 수 없습니다.



변경금지. 귀하는 이 저작물을 개작, 변형 또는 가공할 수 없습니다.

- 귀하는, 이 저작물의 재이용이나 배포의 경우, 이 저작물에 적용된 이용허락조건을 명확하게 나타내어야 합니다.
- 저작권자로부터 별도의 허가를 받으면 이러한 조건들은 적용되지 않습니다.

저작권법에 따른 이용자의 권리는 위의 내용에 의하여 영향을 받지 않습니다.

이것은 [이용허락규약\(Legal Code\)](#)을 이해하기 쉽게 요약한 것입니다.

[Disclaimer](#)

2016년 2월

석사학위 논문

Study of DNA methyltransferase 1
inhibitor RG108 for a preventive
effect of cellular senescence in
human bone marrow
mesenchymal stromal cells

조선대학교 대학원

생명과학과

오 윤 서

Study of DNA methyltransferase 1
inhibitor RG108 for a preventive
effect of cellular senescence in
human bone marrow
mesenchymal stromal cells

DNA 메틸화효소 1 억제제인 RG108의 골수유래
중간엽줄기세포에서의 노화 예방효과에 대한 연구

2016년 2월 25일

조선대학교 대학원

생명과학과

오 윤 서

Study of DNA methyltransferase 1
inhibitor RG108 for a preventive
effect of cellular senescence in
human bone marrow
mesenchymal stromal cells

지도교수 조 광 원

이 논문을 이학석사학위 신청 논문으로 제출함

2015년 10월

조선대학교 대학원

생명과학과

오 윤 서

오윤서의 석사학위논문을 인준함

위원장 조선대학교 부교수 이 준 식 (인)

위 원 조선대학교 조교수 송 상 기 (인)

위 원 조선대학교 부교수 조 광 원 (인)

2015년 11월

조선대학교 대학원

CONTENTS

List of Figures	i
List of Tables	ii
Abbreviations	iii
ABSTRACT	1
국문초록	4
Introduction	7
PART I-I. Introduction	9
PART I-II. Materials and Methods	11
II-1. Characteristics of primary hBM-MSCs and cell culture	11
II-2. Real-time PCR	11
II-3. MTT assay	14
II-4. Immunoblot analysis	14
II-5. Senescence-associated β -galactosidase staining	15
II-6. Wound healing assay	15
II-7. Methylation-specific PCR	16
PART I-III. Result	18

III-1. RG108 induced the expressions of <i>TERT</i> and <i>bFGF</i> in hBM-MSCs	18
III-2. The expressions of the senescence-related factors were shifted in RG108-treated hBM-MSCs	20
III-3. RG108 prevented cellular senescence in hBM-MSCs	22
III-4. RG108 improved cellular migration in hBM-MSCs	24
III-5. RG108 treatment improved protective effects against oxidative stress in hBM-MSCs	26
III-6. RG108 induced the demethylation of the <i>TERT</i> promoter region in hBM-MSCs	28
PART I-IV. Discussion	30
PART II-I. Introduction	33
PART II-II. Materials and Methods	35
II-1. Isolation of ALS-MSCs	35
II-2. Real-time PCR	35
II-3. Immunoblot analysis	38
II-4. Senescence associated β -galactosidase staining	38
II-5. Wound healing assay	39
II-6. MTT assay	39
II-7. Neuronal differentiation	40
PART II-III. Result	41

III-1. Anti-senescence factor expression is modulated by RG108	41
III-2. RG108 treatment of ALS-MSCs prevents cellular senescence	44
III-3. Migration and protection potency are improved in RG/ALS-MSCs	46
III-4. RG/ALS-MSCs effectively differentiate into neuron-like cells	48
PART II-IV. Discussion	51
Conclusion	53
References	54

List of Figures

Introduction

Figure 1. Chemical structure of RG108 8

Part I

Figure 1. RG108 induces the expression of the *TERT* and *bFGF* genes in hBM-MSCs 19

Figure 2. Transcripts of the senescence-related factors were shifted in RG108-treated hBM-MSCs 21

Figure 3. RG108 prevents cellular senescence in hBM-MSCs 23

Figure 4. RG108 improves the cellular migration of hBM-MSCs 25

Figure 5. RG108 improves the protective effects against oxidative stress in hBM-MSCs 27

Figure 6. RG108 induces demethylation at the *TERT* promoter region in hBM-MSCs 29

Part II

Figure 1. RG108 induces the expression of anti-senescence factors in ALS-MSCs 43

Figure 2. RG108 treatment prevents cellular senescence in ALS-MSCs 45

Figure 3. Migration and protective effects were improved in RG108-treated ALS-MSCs 47

Figure 4. Efficiency of neuronal differentiation was increased in RG108-pre treated ALS-MSCs 50

List of Tables

Part I

Table 1. Oligonucleotides used for real-time PCR 13

Table 2. Oligonucleotides used for methylation-specific PCR 17

Part II

Table 1. Oligonucleotides used for real-time PCR 37

Abbreviations

ALS	Amyotrophic lateral sclerosis
ANG	Angiogenin
ATM	Ataxia telangiectasia mutated
bFGF	Basic fibroblast growth factor
BHA	Butylated hydroxyanisole
BM-MSCs	Bone marrow mesenchymal stromal cells
DMSO	Dimethyl sulfoxide
DNMTs	DNA methyltransferases
FBS	Fetal bovine serum
MMPs	Metalloproteinase
MTT	3-(4,5-dimethylthiazol-2-yl)-2,5-diphenyltetrazolium bromide
PBS	Phosphate-buffered saline
PCR	Polymerase chain reaction
RIPA	Radio-immunoprecipitation assay
RT	Room temperature
SFRP1	secreted frizzled-related protein 1
TERT	Telomerase reverse transcriptase
VEGF	Vascular endothelial growth factor

ABSTRACT

Study of DNA methyltransferase 1 inhibitor RG108 for a preventive effect of cellular senescence in human bone marrow mesenchymal stromal cells

Youn Seo Oh

Advisor : Assistant Prof. Goang-Won Cho, Ph.D.

Department of Biology,

Graduate School of Chosun University

Mesenchymal stromal cells (MSCs) are characterized by their multipotency capacity, which allows them to differentiate to diverse cell types, and secrete a variety of trophic factors. These features indicate that MSCs might be of use in stem-cell therapy. However, MSCs undergo cellular senescence during long-term expansion, and this is accompanied by functional declines in stem-cell potency. Recent studies have shown that alteration of DNA methylation is highly associated with cellular senescence and aging-related neurodegenerative disorders, such as amyotrophic lateral sclerosis (ALS).

Remedy of the altered methylation pattern may provide beneficial efficacy in these diseases. In this study, I used a DNA methyltransferase 1 inhibitor, RG108, to investigate the anti-senescence effects in human bone marrow mesenchymal stromal cells (hBM-MSCs). First, I determined the optimized dose and time of RG108 treatment in hBM-MSCs to be 5 μ M for 48 h, respectively. Under these conditions, the anti-senescence genes *TERT*, *bFGF*, *VEGF*, and *ANG* were increased, whereas the senescence-related genes *ATM*, *p21*, and *p53* were decreased. The number of β -galactosidase positive cells was significantly decreased in RG108-treated hBM-MSCs, whereas the rates of cell migration and cellular protection were increased. I have shown that RG108 significantly induces the expression of *TERT* by blocking methylation at the *TERT* promoter region. Thus, these data indicate that an optimized dose of RG108 may improve the cell migration, protection, and cellular senescence, which may provide a better efficacy of these cells in stem cell therapy.

Next, I investigated correlation between excessive DNMT1 expression and functional decline in ALS-patient derived BM-MSCs (ALS-MSCs). The DNMT1 inhibitor RG108 was used for this study. RG108 treated ALS-MSCs exhibit increased expression of the anti-senescence genes *TERT*, *VEGF*, and *ANG*, and decreased expression of the senescence-related genes *ATM*, *p21* and *p53*. The activity of Senescence associated β -galactosidase and the expression of senescence proteins p53 and p16 were reduced in RG108 treated ALS-MSCs. The abilities of cell migration and protection against oxidative damage were improved in the RG108 treated ALS-MSCs. In neuronal differentiation experiments, the RG108 treated ALS-MSCs more effectively

differentiated into neuron-like cells. These results suggest that ALS-MSCs function can be restored by inhibiting excessively expressed DNMT1, an approach that may ultimately provide better efficacy in stem cell therapy.

In the present studies suggest that DNMT1 inhibitor RG108 can improve stem cell potency and, ameliorates cellular senescence in Normal and ALS patients derived BM-MSCs. Which may provide better efficacy in stem cell therapy.

국문초록

DNA 메틸화효소 1 억제제인 RG108의 골수유래 중간엽줄기세포에서의 노화 예방효과에 대한 연구

중간엽줄기세포는 성체줄기세포의 한 종류로, 자기재생산능력(self-renewal)과 다분화능(multipotency)을 가지고 있고, 다양한 영양 인자(trophic factors)들을 분비한다. 그뿐만 아니라, 중간엽줄기세포는 골수, 지방, 탯줄과 같은 조직에서 쉽게 얻을 수 있어서 줄기세포치료에 좋은 도구로 이용되고 있다. 하지만 치료의 효율성을 높이기 위해 개체 수를 늘리는 과정에서 중간엽줄기세포는 점차적인 노화를 겪게 되고, 이는 세포 자체의 기능적인 감소를 야기한다. 인체 내에서, 노화된 줄기세포는 조직 내의 항상성 유지에 부정적인 영향을 미치며, 이러한 상태가 지속되면 대표적인 노인성 질환인 퇴행성 질환의 원인이 된다. 이러한 노화의 분자적인 메커니즘은 여러 연구를 통해 규명되었으며, 최근 연구들에 의하면 노화과정에서 세포 내의 DNA 메틸화(DNA methylation) 패턴에 변형이 일어난다는 것이 알려졌다. 또한, 이는 루게릭병과 같은 노화 관련된 퇴행성 질환과도 밀접한 연관성이 있음이 알려져 있다. 따라서 본 연구에서는, 첫째로 DNA 메틸화효소 억제제로 알려진 RG108의 처리를 통해 인간의 골수 유래 중간엽줄기세포에서의 항-노화 효과를 갖는지 확인하고자 연구를 진행하였다. 먼저, Real-time PCR을 통해 항-노화 관련된 유전자들인 *TERT*와 *bFGF*의 발현을 관찰함에 따라 RG108 처리의 최적 농도와 시간을 5 μ M, 48시간으로 확립하였다. 이 처리 조건에서 항-노화 관련된 유전자들인 *TERT*, *bFGF*, *VEGF* 그리고 *ANG*

가 증가하는 것을 관찰하였고, 반면에 노화 관련된 유전자들인 *ATM*, *p21*, 그리고 *p53*이 감소하는 것을 관찰하였다. 그뿐만 아니라, 세포 수준에서 노화의 정도를 확인할 수 있는 **Senescence associated β -galactosidase staining**을 통해서 세포 수준에서의 항-노화 효과를 관찰하였다. 그다음으로는 이러한 항-노화 효과가 세포의 기능적인 면의 개선에 영향을 미치는지 확인하고자 **Wound healing assay**, **MTT assay**를 실시하여 적절한 조건의 **RG108** 처리는 세포 이동 능력의 향상과 산화스트레스로부터 보호 효과가 있는 것을 확인하였다. 이러한 항-노화 효과의 메커니즘을 확인하기 위해, *TERT* 프로모터의 **DNA** 메틸화 패턴을 조사했을 때, **RG108**에 의해 프로모터의 **DNA** 메틸화가 감소하는 것을 관찰하였다. 따라서 **RG108**은 인간 유래 골수 중간엽줄기세포에서 항-노화 효과를 나타냈고 이는 줄기세포치료의 효율을 증가시키는 데 도움을 줄 것이다.

두 번째 연구에서는 루게릭 환자로부터 추출된 골수 유래 중간엽줄기세포에서, 비정상적으로 증가하여 있는 **DNA** 메틸화 효소 발현과 관련하여 **DNA** 메틸화 효소 억제제인 **RG108**을 처리함에 따른 병리학적인 증상의 개선을 유도할 수 있는지 확인하고자 연구를 진행하였다. 이전의 선행연구로, 루게릭 환자의 중간엽 줄기세포는 정상인의 것에 비하여 기능적으로 감소하여 있다고 보고되었다. 먼저 루게릭 환자의 중간엽줄기세포에서 정상인에 비하여 **DNMT1**의 발현이 비정상적으로 증가하여 있는 것을 관찰하였으며, 이에 따라서 **DNA** 메틸화 효소 억제제인 **RG108**을 처리했을 때, 항-노화 관련된 유전자들인 *TERT*, *VEGF* 그리고 *ANG*가 증가하였고, 반면에 노화 관련 유전자들인 *ATM*, *p21*, *p53*이 감소한 것을 관찰했다. 또한 세포 수준에서 **RG108**이 처리된 루게릭 환자의 줄기세포에서 노화가 개선됨을 관찰하였을 뿐만 아니라, 세포 이동 능력이나 산화스트레스에 대한 보호 효과 또한 증가함을 확인하였다. 그다음으로, 루게릭 환자의 줄기세포를 신경세포로의 분화를 유도한 실험에서, **RG108**을 처리한 뒤 분화를 유도

했을 때, 분화 효율이 증가하는 것을 관찰하였다. 따라서, 루게릭 환자의 중간엽줄기세포의 비정상적으로 발현하는 DNA 메틸화 효소를 RG108을 통해 억제하는 것은 병리학적인 증상을 개선하는 효과를 나타냄을 확인할 수 있었다. 그리고 이는 루게릭 환자의 줄기세포를 이용한 치료에 있어서 도움을 줄 것이다.

이 두 가지 연구는, RG108의 처리는 줄기세포를 이용한 세포 치료법에 있어서 그 효율성을 증가시킬 수 있음을 의미한다.

Introduction

Human mesenchymal stromal cells (MSCs) have differentiation capacity and secrete trophic factors. MSCs can be easily isolated from human bone-marrow, fat, and umbilical-cord tissues. These characteristics provide promise for therapeutic efficacy in stem cell therapy [1, 2]. However, an increasing number of cell divisions for cell therapy increases the risk of cellular senescence, resulting in a reduction in the therapeutic efficacy or failure of cell therapies [5-7].

DNA methylation by DNMT methyltransferases (DNMTs) plays an important role in gene regulation. DNMT1 transfers a methyl group to hemimethylated DNA to maintain methylated DNA [20]. DNMT3A and DNMT3B known as the *de novo* DNA methyltransferases, and are able to transfer methyl group to unmethylated CpGs in DNA [42].

Recent studies have shown that the cellular senescence that occurs during in vitro long-term culture was also caused by epigenetic modification [15, 19], such as DNA methylation [16-18]. Also, aberrant DNA methylation patterns in the genome is associated with various pathological processes and age-related diseases, including cancer, neurodegenerative diseases such as Alzheimer's and Parkinson's diseases, osteoarthritis, type 2 diabetes, renal disease and Amyotrophic lateral sclerosis (ALS) [43, 45, 46, 48, 52].

ALS is a fatal neurodegenerative disease [32]. ALS onset begins with muscle weakness in the arms and legs, and rapidly spreads to other regions, causing problems in speech, swallowing, and breathing [33]. Recent studies

have shown that ALS are not only restricted to motor neuron, but also affect human bone marrow mesenchymal stem cells (hBM-MSCs). For instance, alterations in metalloproteinase (MMPs), and decreased stem cell capacities in BM-MSCs [7, 36] have all been observed in ALS patients. The cause of ALS is not known clearly. However, several recent studies have reported aberrant DNA methylation in ALS patients [35, 48, 52].

RG108 (Fig. 1), a non-covalent DNMT1 inhibitor, binds at the micromolar range to the DNMT1 pocket site and blocks DNA binding [23, 24].

In this study, I investigated the effect of DNMT1 inhibition in hBM-MSCs and ALS patients derived BM-MSCs (ALS-MSCs), and observed the functional restoration by anti-senescence effect.

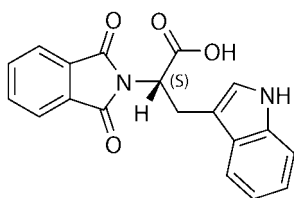


Figure 1. Chemical structure of RG108

PART I.

Anti-senescence effects of DNA methyltransferase inhibitor RG108 in human bone marrow mesenchymal stromal cells

I. Introduction

Human bone marrow mesenchymal stromal cells (hBM-MSCs) have been used in stem cell therapies for various diseases [1, 2]. However, it is difficult to obtain a sufficient amount of stem cells owing to their poor isolation yield from donors. In order to obtain a sufficient quantity of stem cells, most researchers expand the yield of isolated stem cells under in vitro culture conditions. However, studies have shown that hBM-MSCs cultured over a long term will undergo cellular senescence, with telomere shortening and a decline of telomerase (TERT) activity [3, 4].

DNA methylation plays a crucial role in the regulation of a variety of biological processes, including the regenerative capacity [8, 9] and self renewal [10] of stem cells. Aberrant DNA methylation induced by intrinsic or extrinsic factors may lead to an alteration of the cellular phenotypes and increase the risk for certain physical diseases, such as cancer [11, 12], and degenerative diseases [13, 14].

Recent studies have shown that the senescence phenotype is brought on by increased epigenetic modifications [15], as results in the formation of

senescence-associated heterochromatin foci [16-18], which can also be initiated by DNA methylation. This suggests that stem cells, applied to therapy in particular, have to be managed for epigenetic modifications during cell clonal expansion.

DNA methyltransferases (DNMTs) are known to be major epigenomic modulators. DNA methylation was catalyzed by DNMT3A and 3B de novo, and the methylation of hemimethylated DNA was subsequently maintained by DNMT1 [20]. There is also growing evidence that the activities of DNMTs are associated with ageing and ageing-related diseases [16, 21].

In this study, I investigated the effects of RG108 on stem cell senescence and identified its mechanism of action.

PART I-II. Materials and Methods

II-1. Characteristics of primary hBM-MSCs and cell culture

The hBM-MSCs were purchased from CEFO (Cell Engineering For Origin, Korea). The cells were examined for viral infection and mycoplasma contamination, and all presented as negative. Flow cytometric analysis of the cells revealed a CD73⁺, CD105⁺, CD31⁻ phenotype. The hBM-MSCs were cultured in T75 flasks (Becton Dickinson, USA) according to the supplier's recommendations. Cells were cultivated in hBM-MSC growth medium (Gibco, USA), containing 10% FBS, l-glutamine, penicillin, and streptomycin, without any stimulatory supplements or vitamins. Cells were maintained in a humidified incubator at 37°C, using a standard mixture of 95% air and 5% CO₂. Seven-passage hBM-MSCs were used for these experiments.

II-2. Real-time PCR

hBM-MSCs were seeded in 100mm-dish (5×10^4 cells/dish) and incubated at 37°C for 2 days. Cells were then treated with 0~10 μ M RG108 for 0~72 h. Cells were harvested and the total RNAs extracted using RNA iso reagent (TAKARA, Japan) according to the manufacturer's instructions. The Primescript II 1st strand cDNA synthesis kit (TAKARA, Japan) was used to reverse transcribe 3~5 μ g of total RNA with 5 μ M of Oligo (dT) primers (TAKARA, Japan), 1 mM each dNTP, and the supplied buffer. First-strand cDNAs were

amplified using the Power SYBR Green PCR master mix (Applied Biosystems Inc., USA) with gene-specific primers for human *ANG*, *ATM*, *bFGF*, *p21*, *p53*, *TERT*, *VEGF*, or *β -actin*. The real-time PCR cycling parameters were as follows: 95°C for 10 min, followed by 40 cycles of 15 s at 95°C, and 1 min at 60°C. The primers were synthesized by GenoTech (GenoTech Corp., Korea) and IDT (Integrated DNA Technologies Inc., USA) and are summarized in Table 1. ABI step one real-time PCR system was used (Applied Biosystems Inc., USA).

Table 1. Oligonucleotides used for real-time PCR

Gene	Forward primer (5' → 3')	Reverse primer (5' → 3')	Acc. No.
<i>bFGF</i>	AAAAACGGGGGCTTCTTCCT	ACGGTTAGCACACACTCCTT	NM_002006
<i>TERT</i>	ATGCCAGCATCATCAAACC	GGTAGAGACGTGGCTCTTGA	NM_198253.2
<i>Oct4</i>	GCCCGAAAGAGAAAGCGAAC	AACCACACTCGGACCACATC	NM_002701
<i>VEGF</i>	AGAAAATCCCTGTGGGCCTT	GTCACATCTGCAAGTACGTTG	NM_001025368
<i>ANG</i>	TGGGCGTTTTGTTGTTGGTC	GGCATCATAGTGCTGGGTCA	NM_001145
<i>ATM</i>	GGAAGAGATGTGTAAGCGCA	GAGAAAAGCTCCCCAATGCT	NM_000051.3
<i>p21</i>	GTCTTGACCCTTGTGCCTC	GGCGTTGGAGTGGTAGAAA	NM_000389.4
<i>p53</i>	AGGAAATTTGCGTGTGGAGT	AGTGGATGGTTGTACAGTCA	NM_000546
<i>β-actin</i>	ATCCGCAAAGACCTGTACGC	TCTTCATTGTGCTGGGTGCC	NM_001101

Acc. No. indicates gene access number.

II-3. MTT assay

The protective effects against H₂O₂-induced oxidative stress were measured by MTT assay (Sigma, USA) according to the manufacturer's instructions. Briefly, 2.5 x 10³ hBM-MSCs were seeded into 96-well plates. On the next day, the cells were incubated with/without 5 μM RG108 for 48 h, treated with 0~1.5 mM H₂O₂ for 1.5 h, and then subjected to MTT assay.

For examination of cell toxicity effect by RG108 (dissolved in DMSO), Cells were incubated with several concentrations (0~10 μM) of RG108 for 48 h and then measured by MTT assay.

For testing the effect of RG108 on the cell proliferation rate, Cells were treated with/without 5 μM RG108 for 48 h. After that, the cells were washed, replenished with normal growth medium, and then further incubated for 24 or 48 h before being subjected to the MTT assay.

II-4. Immunoblot analysis

Cells were seeded in 100mm-dish (5 x 10⁴ cells/dish) and incubated at 37°C for 2 days. Cells were then treated with 5 μM RG108 for 48 h. The cells (3 x 10⁵) were extracted with 40 μL of RIPA buffer containing protease and phosphatase inhibitors (Santa Cruz Biotechnology, USA) for 30 min at 4°C, and then centrifuged at 16,000 x *g* for 20 min. The total proteins were then subjected to immunoblotting with antibodies to TERT (1:500), p53 (1:500), ATM (1:5,000), p21 (1:500), cleaved caspase-3 (1:200), or β-actin (1:5,000),

and subsequently to the appropriate horseradish-peroxidase-conjugated secondary antibodies (1:10,000; Jackson ImmunoResearch Laboratories, USA). The western blots were quantified with the Image J program.

II-5. Senescence-associated β -galactosidase staining

Senescence-associated β -galactosidase (SA- β -gal) staining was carried out using the Senescence β -Galactosidase Staining kit (Cell Signaling Technology Inc., USA) according to the manufacturer's instructions. The hBM-MSCs were seeded into 6-well plates at a density of 1×10^4 cells/well and incubated until the appropriate confluence was reached. The cells were washed with PBS and fixed with 2% formaldehyde and 0.2% glutaraldehyde in distilled water for 15 min at room temperature. The cells were then washed twice with PBS containing 1 mM $MgCl_2$ (pH 7.2) and stained overnight in β -galactosidase staining solution {1 mg/mL X-gal, 5 mM $K_3Fe[CN]_6$ (potassium ferricyanide), 5 mM $MK_4Fe[CN]_6$ (potassium ferrocyanide), 2 mM $MgCl_2$, 40 mM citric acid/sodium phosphate (pH 6.0), and 150 mM NaCl in distilled water} at 37°C without CO_2 . Images were captured with a microscope (Canon, Japan). The results were presented as the means of four independent experiments.

II-6. Wound healing assay

hBM-MSCs were seeded into 6-well plates and incubated overnight in standard growth medium at 37°C and 5% CO_2 . A uniform scratch was made

in the 100% confluent monolayer culture. The wound was introduced by scraping the monolayer with a sterile 200 μ L pipette tip and then washing the monolayer with growth medium to remove cell debris. The cells were then replenished with fresh growth medium, and wound closure was documented by photography of the same region at different times (0~18 h). Migration cells were counted at each time point (0~18 h). The results were presented as the means of four independent experiments.

II-7. Methylation-specific PCR

Methylation-specific PCR primers were designed for the upstream (~600 bp from transcription start site) and downstream regions (encompassing the transcription and translation start sites) of the *TERT* promoter [24]. PCRs were performed with 25 ng of bisulfite-treated DNA and *Taq* DNA polymerase (Bioneer, Korea). The PCR cycling parameters were as follows: initial denaturation at 94°C for 1 min; 40 cycles of 30 s at 94°C for denaturation, 30 s at 60°C for primer annealing, 30 s at 72°C for extension, and a final extension at 72°C for 3 min. The PCR products were analyzed by 2% agarose gel electrophoresis and quantified with the Image J program. The primers were synthesized by GenoTech (GenoTech Corp., Korea) and are summarized in Table 2. ABI 2720 Thermal Cycler was used (Applied Biosystems Inc., USA).

Table 2. Oligonucleotides used for methylation-specific PCR [24]

Names		Sequence (5' → 3')
Promoter	Forward	: GAG GTA TTT CGG GAG GTT TCG C
upregion M	Reverse	: ACT CCG AAC ACC ACG AAT ACC G
Promoter	Forward	: GGG AGG TAT TTT GGG AGG TTT TGT
upregion U	Reverse	: CAA ACT CCA AAC ACC ACA AAT ACC A
Promoter	Forward	: GGT TTC GTT TTT TTT TTG CGG C
downregion M	Reverse	: GAC TCG ACA ACG AAA AAC GCG
Promoter	Forward	: TTG TGG TTT TGT TTT TTT TTT GTG GT
downregion U	Reverse	: ACA CAC AAC TCA ACA ACA AAA AAC ACA

PART I-III. Result

III-1. RG108 induced the expressions of *TERT* and *bFGF* in hBM-MSCs

To evaluate the concentration effects of RG108, hBM-MSCs were incubated with 0, 1, 5, or 10 μM of RG108 for 48 h. The expressions of *bFGF* and *TERT* were assessed by real-time PCR and the maximum expressions were identified to be in 5 μM RG108-treated hBM-MSCs (Fig. 1A; *t*-test, $*p < 0.05$, mean \pm SD, $n=3$). To determine the optimal treatment time of RG108 in hBM-MSCs, Cells were incubated with 5 μM RG108 for several incubation times (0~72 h). As shown in Fig. 1B, transcripts of the tested genes were maximal at 48 h of incubation (Fig. 1B; *t*-test, $*p < 0.05$, mean \pm SD, $n=3$). There were no differences in cell viability between treated and untreated (control) hBM-MSCs under the tested conditions (Fig. 1C). From these data, I determined the optimized treatment condition in hBM-MSCs to be 5 μM RG108 for 48 h.

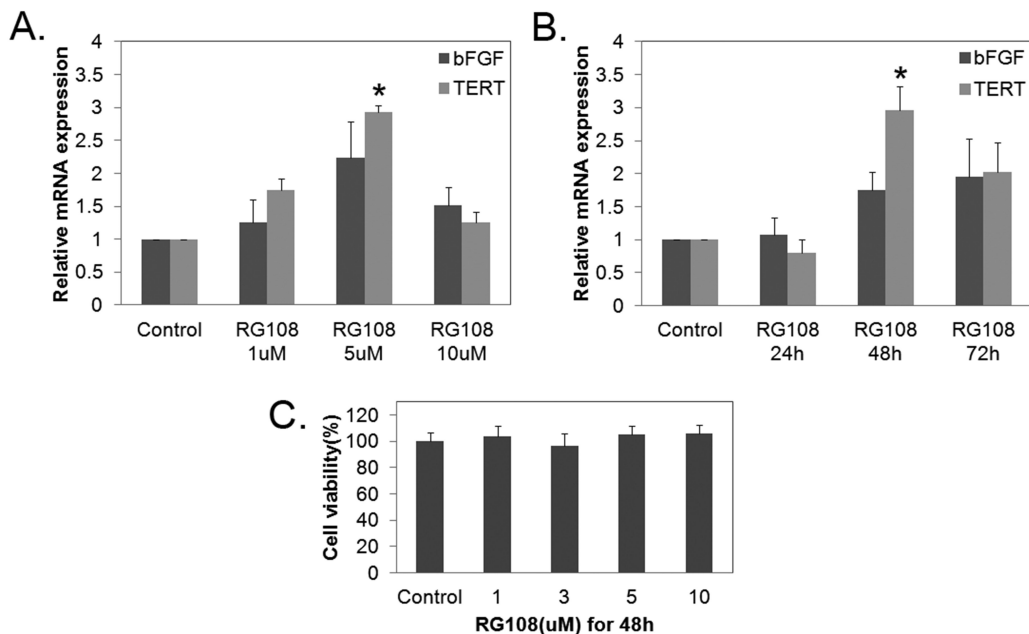


Figure 1. RG108 induces the expression of the *TERT* and *bFGF* genes in hBM-MSCs.

(A) The increased expressions of *bFGF* and *TERT* in hBM-MSCs treated with RG108 (0~10 μ M) were measured by real-time PCR. (B) The expressions were maximal at 48 h incubation with 5 μ M RG108 treatment, as measured by real-time PCR. (C) No cytotoxicity was observed in the determined conditions, as tested by MTT assay.

III-2. The expressions of the senescence-related factors were shifted in RG108-treated hBM-MSCs.

I have shown that RG108 stimulates the expression of anti-senescence factors at the determined conditions. To further investigate the role of RG108, various senescence- or anti-senescence related genes were examined by real-time PCR. Transcripts of the anti-senescence genes *TERT*, *bFGF*, *VEGF*, and *ANG* [7, 25] were significantly increased in RG108-treated hBM-MSCs (RG108-MSCs), whereas the senescence genes *ATM*, *p21*, and *p53* were decreased compared with non-treated hBM-MSCs (Control-MSCs) (Fig. 2A; *t*-test, * $p < 0.05$, # $p < 0.01$, mean \pm SD, $n=4$). The expression of *TERT* was increased up to 3.2-fold. To confirm the real-time PCR results at the protein level, immunoblot analysis was performed with antibodies against TERT, p53, ATM, p21, and β -actin, and the obtained results were consistent with Figure 2A (Fig. 2B and 2C; *t*-test, * $p < 0.05$, mean \pm SD, $n=3$).

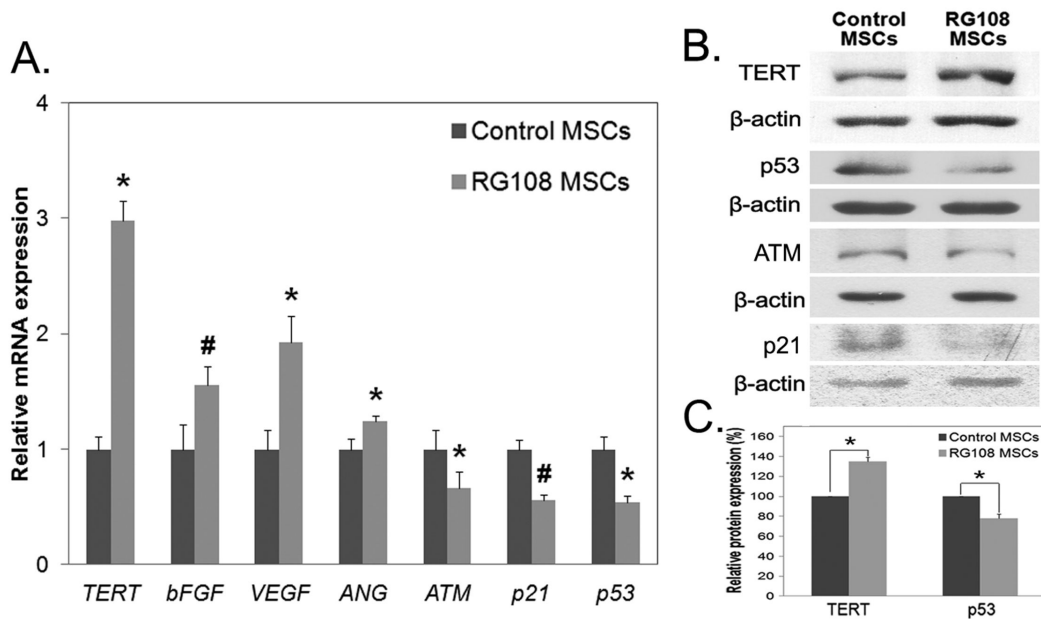


Figure 2. Transcripts of the senescence-related factors were shifted in RG108-treated hBM-MSCs.

(A) The expressions of anti-senescence factors *TERT*, *bFGF*, *VEGF* and *ANG* were significantly increased, whereas those of senescence factors *ATM*, *p21* and *p53* were significantly decreased in RG108-MSCs, as measured by real-time PCR. (B) The expressions were confirmed by immunoblot analysis with TERT, p53, ATM, p21, or β-actin specific antibodies. (C) The data were quantified by using the Image J software.

III-3. RG108 prevented cellular senescence in hBM-MSCs

From this study, I have shown that senescence-related factors were modulated following RG108 treatment. To confirm this effect at the cellular level, SA- β -gal assays were performed on hBM-MSCs in the absence or presence of RG108 (5 μ M, 48 h) (Fig. 3A). The number of SA- β -gal stained cells in RG108-MSCs was decreased 17.8% compared with control-MSCs (100%). (Fig. 3B; *t*-test, **p*<0.05, mean \pm SD, n=4).

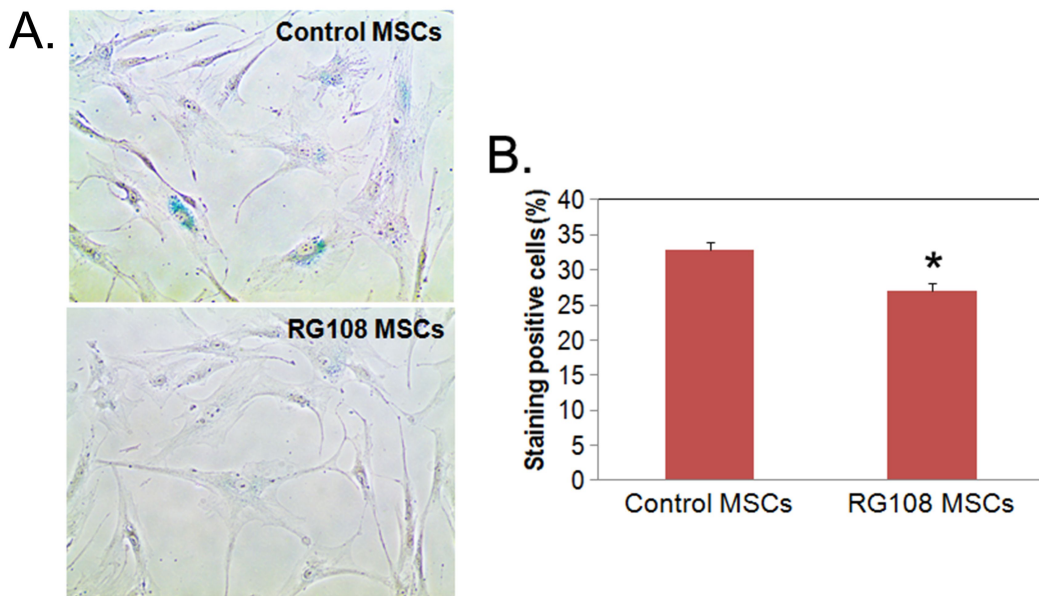


Figure 3. RG108 prevents cellular senescence in hBM-MSCs.

(A) SA β -gal staining assays were performed in RG108-treated (RG108-MSCs) or non-treated hBM-MSCs (Control-MSCs). The senescent cells are indicated by the blue-stained cells. (B) The number of total cells and senescent cells (blue color) were counted and the results are presented graphically.

III-4. RG108 improved cellular migration in hBM-MSCs

The migratory ability of stem cells is also an important factor for stem cell potency. This study has presented that RG108 induces the expression of several trophic factors, including *ANG* and *VEGF* (Fig. 2), which stimulate cell migration. To examine the migratory effects of RG108, hBM-MSCs were seeded into well plates and incubated with/without 5 μ M RG108 for 48 h. Cells were then subjected to the wound healing assay (Fig. 4A). Increased migration rates were observed in RG108-MSCs (Fig. 4B; *t*-test, **p*<0.05, mean \pm SD, n=4). The rate of cell proliferation was unchanged at the designed condition (Fig. 4C; mean \pm SD, n=3), indicating that the increased migration in RG108-MSCs was not due to increased cell proliferation.

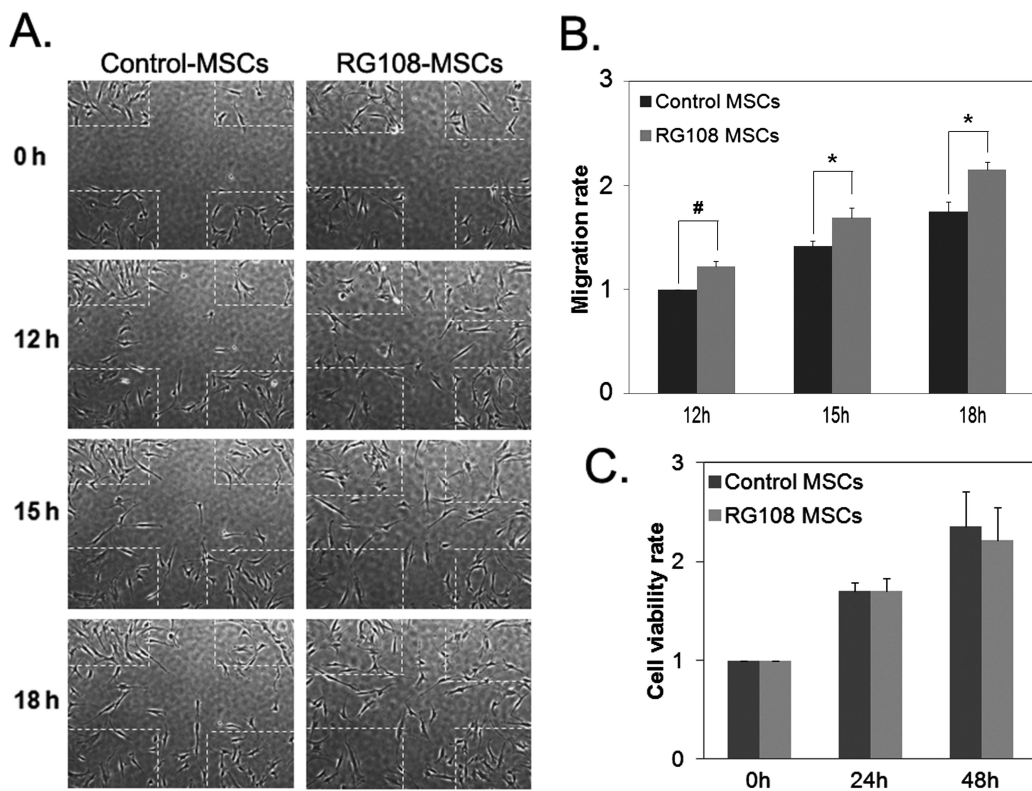


Figure 4. RG108 improves the cellular migration of hBM-MSCs.

(A) The migration of RG108-treated hBM-MSCs was observed for 18 h after being scratched (inside dotted line). (B) Migrated hBM-MSCs inside the dotted lines were counted. (C) Cell proliferation was not affected by RG108, as measured by MTT assay.

III-5. RG108 treatment improved protective effects against oxidative stress in hBM-MSCs

Since RG108 increased the expression of anti-senescence factors in hBM-MSCs, I examined the cell protective effect of this enzyme inhibitor. RG108-pretreated hBM-MSCs were exposed to H₂O₂ (0~1.5 mM) for 1.5 h and then subjected to cell viability assay. The viability of RG108-MSCs was significantly increased 108.8% compared with control-MSCs (100%) under the oxidative stress (1 mM H₂O₂ for 1.5 h). (Fig 5A; *t*-test, **p*<0.05, #*p*<0.01, mean ± SD, n=7). Consistent results were obtained in immunoblot analysis with anti-cleaved caspase-3 antibody (Fig. 5B). This result indicates that cellular damage due to oxidative stress was alleviated by the pre-incubation with low-dose RG108.

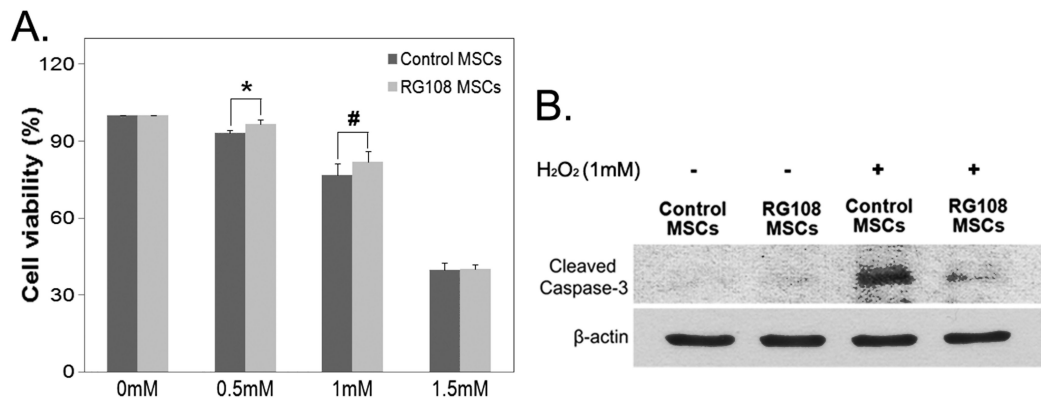


Figure 5. RG108 improves the protective effects against oxidative stress in hBM-MSCs.

(A) RG108-pretreated hBM-MSCs were exposed to 0~1.5 mM H₂O₂ and the cell viabilities were examined by MTT assay. (B) RG108-MSCs were exposed to 1 mM H₂O₂ and subjected to immunoblot analyses with anti-cleaved caspase-3 antibody.

III-6. RG108 induced the demethylation of the *TERT* promoter region in hBM-MSCs

RG108 significantly induced the *TERT* expression, resulting in the anti-senescence phenotype. To assess the methylation status at the *TERT* promoter region, I performed the methylation-specific PCR. The genomic DNA from RG108-MSCs and Control-MSCs were modified with bisulfate and amplified with methylation- or demethylation-specific primers for the *TERT* promoter region [24] (Fig. 6A and 6B). Control-MSCs were partially demethylated at either the promoter upstream region (~600 bp from transcription start site) or promoter downstream region (encompassing the transcription and translation start sites) of the *TERT* promoter, whereas the demethylation status was much greater in RG108-MSCs (Fig. 6C; *t*-test, * $p < 0.05$, mean \pm SD, $n=3$). The demethylation by RG108 was more severe at the promoter downstream region.

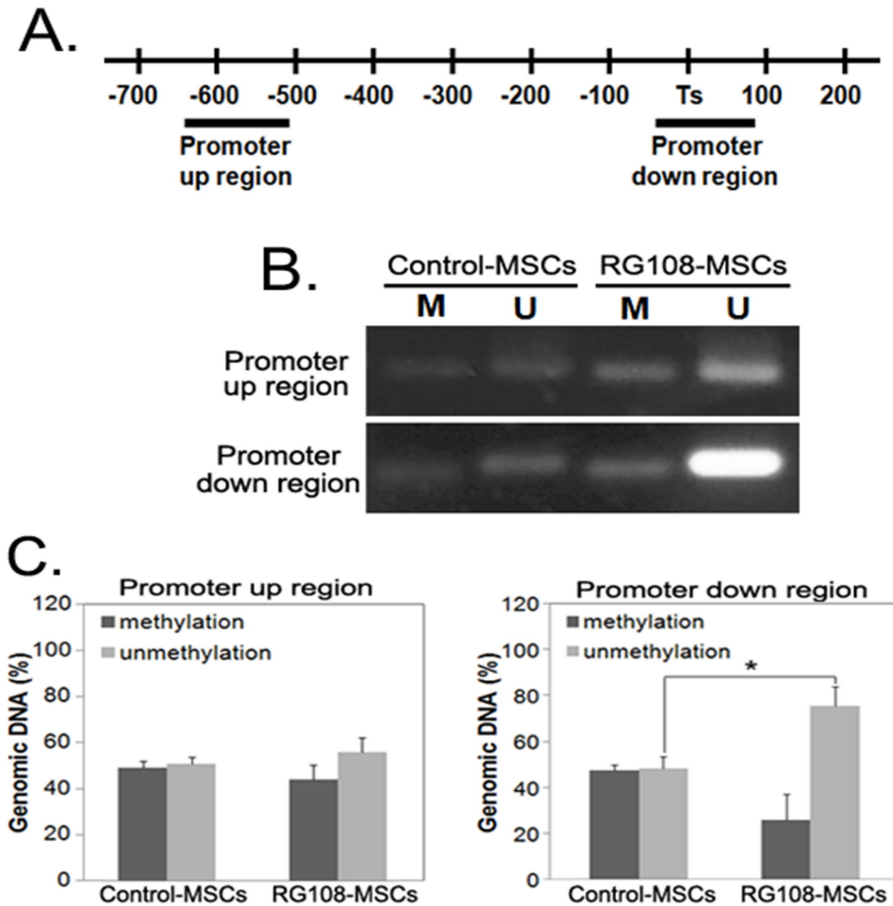


Figure 6. RG108 induces demethylation at the *TERT* promoter region in hBM-MSCs.

(A) Schematic diagram of the *TERT* promoter regions. Ts indicates transcription start site. (B) Methylation-specific PCRs were performed with specific primers of the *TERT* promoter upstream or downstream regions. RG108 induced demethylation at both the *TERT* promoter upstream and downstream regions. M, methylation; U, demethylation. (C) The bands were quantified using the Image J software.

PART I-IV. Discussion

Recent studies have proved that cellular senescence during clonal expansion occurs by epigenetic modifications [15, 19]. In this study, I treated hBM-MSCs with the DNMT1 inhibitor RG108 and identified the increased expression of senescence-associated genes *bFGF*, *TERT*, *VEGF*, and *ANG* and the decreased expression of senescence genes *ATM*, *p21*, and *p53* in the treated cells (Fig. 2A). The increased expression of *TERT*, which plays a key role in telomere shortening during the progression of cellular senescence, was confirmed by immunoblot analysis (Fig. 2B and 2C). These results propose the possibility of anti-senescence effects by RG108 at the optimized condition of RG108 treatment.

The transcriptional modulation of senescence-associated genes by RG108 may attenuate the cellular senescence in hBM-MSCs. To examine this, SA- β -gal assays were performed on RG108-treated hBM-MSCs. The number of senescent cells was lower in RG108-MSCs than in the Control-MSCs (Fig. 3).

Migration ability is also an important factor for stem cell potency. In cell therapy, injected stem cells have been shown to migrate toward the site of injured cells [26]. I have shown that RG108 induces the expression of the migratory markers *VEGF* and *ANG*, suggesting that RG108 treatment may improve the hBM-MSCs migratory ability. As shown in Figure 4, RG108 treatment increased the migration ability of the hBM-MSCs (Fig. 4A and 4B). Thus, RG108 ameliorates cellular senescence by the transcriptional modulation of senescence-associated genes.

Increases in the intracellular level of reactive oxygen species caused by DNA damage can induce the senescence-associated serial proteins ATM and p53 [27]. Since I have shown that RG108 decreases the expression of pro-senescence genes in hBM-MSCs (Fig. 2), RG108-MSCs may have acquired protective effects against the damage induced by oxidative stress. To examine this, cell viability assays were performed, which showed that RG108 alleviated the damage induced by oxidative stress in hBM-MSCs (Fig. 5).

One of the processes in human aging is the progressive attrition of telomeres [28]. Experiments using telomerase-deficient mice showed that accelerated telomere shortening would eventually lead to a limitation of the mouse's longevity [29, 30]. Another study showed that long-term cultured hBM-MSCs, with increases in both the expression of the anti-senescence proteins and the percentage of aneuploid cells, were rescued by transduction of the *TERT* gene [31]. In this study, I have shown that RG108 significantly induces the expression of *TERT*, following blocking of methylation at the *TERT* promoter region (Fig. 6), resulting in amelioration of the senescence phenotype (Fig. 3~5).

Previous reports have shown that the treatment of RG108 at a high micromolar concentration (100 μ M) induces cell cycle arrest and the re-expression of anticancer genes (senescence proteins) p16, SFRP1 (secreted frizzled-related protein 1), and TIMP-3 (metalloproteinase-3) in cancer cells [22]. In this study, I have shown that a low micromolar concentration of RG108 (5 μ M) stimulated the expression of anti-senescence genes (Fig. 2), whereas high-dose RG108 did not (Fig. 1A). These differences between the

previous study and me may be due to the use of different RG108 concentrations, which have varying effects on the methylation of genomic DNA. In addition, I have used primary cultured hBM-MSCs for this study.

I have described the anti-senescence effects in RG108-treated hBM-MSCs. However, there are limitations to this study in that I was unable to confirm whether this modulation is direct or not. Based on the functional mechanism of RG108 as a DNA methyltransferase 1 inhibitor, which blocks DNMT1, it is possible that RG108 induction acts to increase the number of demethylated cytosine residues in the genomic DNA, thereby activating many gene loci and regulating the expression of various genes. Therefore, global genomic analysis of RG108-MSCs may provide a better picture of how the global genes are remodulated by RG108, which may provide the clues to understanding the overall mechanisms of RG108.

PART II.

Functional Restoration of Amyotrophic Lateral Sclerosis Patient-Derived Mesenchymal Stromal Cells Through Inhibition of DNA Methyltransferase

I. Introduction

Amyotrophic lateral sclerosis (ALS) is a fatal neurodegenerative disease characterized by progressive motor neuron death [32]. Most ALS patients die within 3–5 years from the onset of early symptoms [33]. However, Recent studies have shown that pathological abnormalities in ALS are not only restricted to the nervous system, but can also affect other systems, such as hBM-MSCs [7].

hBM-MSCs are multipotent and can, thus, differentiate into diverse cell types [37-39]; they secrete various trophic/growth factors which contribute to stem cell differentiation, cellular protection against stress, and proliferation [1, 7, 25]. hBM-MSCs have been used in preclinical research for cell therapy in diverse degenerative diseases including neurological disorders such as ALS [40, 41]. However, previous study demonstrated that BM-MSCs isolated from ALS patients (ALS-MSCs) have diminished capacity for secreting a variety of trophic/growth factors, resulting in reduced migration ability [7]. This suggests that BM-MSCs from ALS patients may require improvement prior to use in

autologous cell therapy.

DNA methylation, mediated largely by DNA methyltransferases (DNMTs), plays an important role in gene expression. In ALS patients, increased expression of DNMT1 and DNMT3A has been observed in motor cortex tissues and spinal cord motor neurons [47]. Elevated global DNA methylation was also observed in the whole blood of ALS patients [35, 48]. Not unlike progressive degenerative diseases, cellular senescence is brought on by increased epigenetic modifications, driving DNA methylation-induced formation of senescence-associated heterochromatin foci [16-18]; this suggests that there may be a symptomatic correlation between cellular senescence and degenerative diseases, like ALS, at the epigenetic level.

In this study, I investigated the effect of DNMT1 inhibitor RG108 in ALS-MSCs and observed the prevention of cellular senescence and recovery of neural differentiation capacity.

PART II-II. Materials and Methods

II-1. Isolation of ALS-MSCs

Four remnant and stored ALS patient-derived BM-MSCs from a previous investigational clinical trial [50] approved by the Institutional Review Board (HYUH IRB 2006-339) and the Korean Food and Drug Association (KFDA, Bio-47) were used in this study. The protocol for ALS-MSC isolation and culture was described previously [50]. Briefly, mononuclear cells were isolated by bone marrow aspiration at the iliac crest and subjected to a density gradient (Histopaque, density 1.077 g/mL; Sigma, USA). Cells were seeded at a density of 2×10^5 cells/cm² and cultured in DMEM-LG with 10% FBS at 37°C in 5% CO₂ for 3 days. After removing non-adherent cells, the culture medium was changed twice per week. For passage, cells were detached with 0.25% trypsin/ethylene diamine tetraacetic acid for 3 min at 37°C, seeded at a density of 4×10^3 cells/cm², and expanded up to 80–90% confluence. Cell immunophenotype was confirmed by flowcytometry. Three normal hBM-MSC lines were purchased from Lonza (Lonza, USA) and CEFO (Cell Engineering For Origin, Korea). Seven-passage cells were used for these experiments.

II-2. Real-time PCR

Cells were harvested and total RNA was extracted using RNAiso reagent (TAKARA, Japan) according to the manufacturer's instructions. The Primescript

II 1st strand cDNA synthesis kit (TAKARA, Japan) was used to reverse transcribe 3–5 µg of total RNA with 5 µM Oligo (dT) primers (TAKARA, Japan), 1 mM each dNTP, and the supplied buffer. First-strand cDNAs were amplified using Power SYBR Green PCR master mix (Applied Biosystems Inc., USA) with gene-specific primers for human *ANG*, *ATM*, *p21*, *TERT*, *VEGF*, *DNMT1*, *DNMT3A*, *DNMT3B*, or *β-actin*. The real-time PCR cycling parameters were as follows: 95°C for 10 min, followed by 40 cycles of 15 s at 95°C, and 1 min at 60°C. The primers were synthesized by GenoTech (GenoTech Corp., Korea) and IDT (Integrated DNA Technologies Inc., USA) and are summarized in Table 1.

Table 1. Oligonucleotides used for real-time PCR

Gene	Forward primer (5' → 3')	Reverse primer (5' → 3')	Acc. No.
<i>DNMT1</i>	CTGTACCGAGTTGGTGATGG	TAGTGCTCTGGGTACAGGTC	NM_001130823.1
<i>DNMT3A</i>	AGACGGCAAATTCTCAGTGG	GTAGATGGCTTTGCGGTACA	NM_022552.4
<i>DNMT3B</i>	CCCATGCAACGATCTCTCAA	TTGGGGCGTGAGTAATTCAG	NM_006892.3
<i>TERT</i>	ATCGCCAGCATCATCAAACC	GGTAGAGACGTGGCTCTTGA	NM_198253.2
<i>ANG</i>	TGGGCGTTTTGTTGTTGGTC	GGCATCATAGTGCTGGGTCA	NM_001145
<i>VEGF</i>	AGAAAATCCCTGTGGGCCTT	GTCACATCTGCAAGTACGTTCCG	NM_001025368
<i>ATM</i>	GGAAGAGATGTGTAAGCGCA	GAGAAAAGCTCCCCAATGCT	NM_000051.3
<i>p21</i>	GTCTTGTACCCTTGTGCCTC	GGCGTTTGGAGTGGTAGAAA	NM_000389.4
<i>β-actin</i>	ATCCGCAAAGACCTGTACGC	TCTTCATTGTGCTGGGTGCC	NM_001101

Acc. No. indicates gene access number.

II-3. Immunoblot analysis

Protein was extracted from cells with 40 μ L of RIPA buffer containing protease and phosphatase inhibitors (Santa Cruz Biotechnology, USA) for 30 min at 4°C, and then centrifuged at 16,000 $\times g$ for 20 min. 30 μ g of total proteins were then subjected to immunoblotting with antibodies to DNMT1 (1:500), TERT (1:500), p53 (1:500), p16 (1:500), ANG (1:500), Nestin (1:500), Tuj-1 (1:500), or β -actin (1:5000) for overnight at 4°C, and subsequently to the appropriate horseradish-peroxidase-conjugated secondary antibodies (1:10,000; Jackson ImmunoResearch Laboratories, USA) for 2 h at room temperature. Primary antibody for β -actin was used as protein loading control. The western blots were quantified with the Image J program.

II-4. Senescence associated β -galactosidase staining

SA- β -gal staining was carried out using the Senescence β -Galactosidase Staining kit (Cell Signaling Technology Inc., USA) according to the manufacturer's instructions. The ALS-MSCs were seeded into 6-well plates at a density of 1×10^4 cells/well and incubated until the appropriate confluence (70~80%) was reached. The cells were washed with PBS and fixed with 2% formaldehyde and 0.2% glutaraldehyde in distilled water for 15 min at room temperature. The cells were then washed twice with PBS containing 1 mM $MgCl_2$ (pH 7.2) and stained overnight in β -galactosidase staining solution {1 mg/mL X-gal, 5 mM $K_3Fe[CN]_6$ (potassium ferricyanide), 5 mM $K_4Fe[CN]_6$

(potassium ferrocyanide), 2 mM MgCl₂, 40 mM citric acid/sodiumphosphate (pH 6.0), and 150 mM NaCl in distilled water} at 37°C without CO₂. Images were captured with a microscope (Canon, Japan). The results are presented as the means of four independent experiments.

II-5. Wound healing assay

ALS-MSCs were seeded into 6-well plates and incubated overnight in standard growth medium at 37°C and 5% CO₂. A uniform scratch was made in the 100% confluent monolayer culture. The wound was introduced by scraping the monolayer with a sterile 200 µL pipette tip and then washing the monolayer with growth medium to remove cell debris. The cells were then replenished with fresh growth medium, and wound closure was documented by photography of the same region at different times (0~18 h). Migration cells were counted at each time point (0~18 h). The results were presented as the means of four independent experiments.

II-6. MTT assay

The protective effects against H₂O₂-induced oxidative stress were measured by MTT assay (Sigma, USA) according to the manufacturer's instructions. Briefly, 2.5 × 10³ ALS-MSCs were seeded into 96-well plates. On the following day, the cells were incubated with/without 5 µM RG108 for 48 h, treated with 0~1.5 mM H₂O₂ for 1.5 h, and then subjected to MTT assay.

II-7. Neuronal differentiation

ALS-MSCs were incubated with/without 5 μ M RG108 for 48 h. The cells were then exposed to pre-induction medium containing DMEM, 10% FBS, 10 ng/mL bFGF, and 500 μ M β -mercaptoethanol for 24 h. The medium was then replaced with induction medium containing 100 μ M butylated hydroxyanisole (BHA) and 2% dimethyl sulfoxide (DMSO) in FBS-free medium for 6 h, according to previously described procedures [37, 51]. Control ALS-MSCs were incubated with FBS-containing medium for 24 h. The medium was replaced with FBS-free medium and the cells were incubated for an additional 6 h. Images were captured with a digital camera (Canon, Japan). Neurite lengths were measured using the Image J program.

PART II-III. Result

III-1. Anti-senescence factor expression is modulated by RG108

The expression of DNMT1 is 2.28-fold higher in BM-MSCs isolated from ALS patients (ALS-MSCs) than in normal hBM-MSCs (Nor-MSCs) (Fig. 1A; Mann-Whitney *U*-test, #*p*<0.01, mean ± SD, n=3, 4). Similar results were obtained by immunoblot analysis of DNMT1 proteins (174% versus Nor-MSCs) (Fig. 1B; Mann-Whitney *U*-test, **p*<0.05, mean ± SD, n=3, 4).

The DNMT1 inhibitor RG108 (5 μM, 48 h) was used to examine the effects of DNMT1 inhibition in ALS-MSCs. The expression of the anti-senescence genes was significantly increased by 1.65-fold (*TERT*), 1.25 (*VEGF*) and 1.29 (*ANG*), whereas the expression of the senescence genes was decreased by 0.67 (*ATM*), 0.82 (*p21*) and 0.79 (*p53*) in RG108-treated ALS-MSCs (RG/ALS-MSCs) compared to non-treated ALS-MSCs (Fig. 1C; *t*-test, **p*<0.05, #*p*<0.01, mean ± SD, n=4). Immunoblot analysis with antibodies specific to *TERT* and *ANG* yielded consistent results (120% for *TERT*, 123% for *ANG*). (Fig. 1D; *t*-test, **p*<0.05, mean ± SD, n=4).

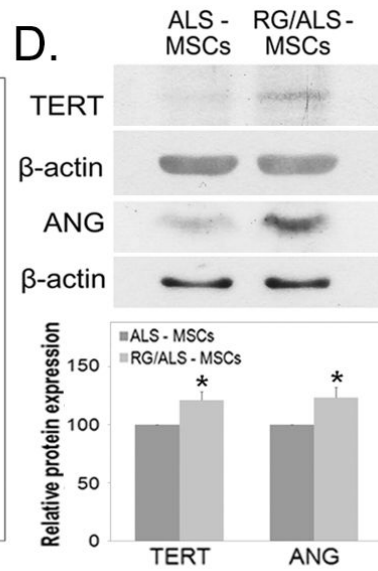
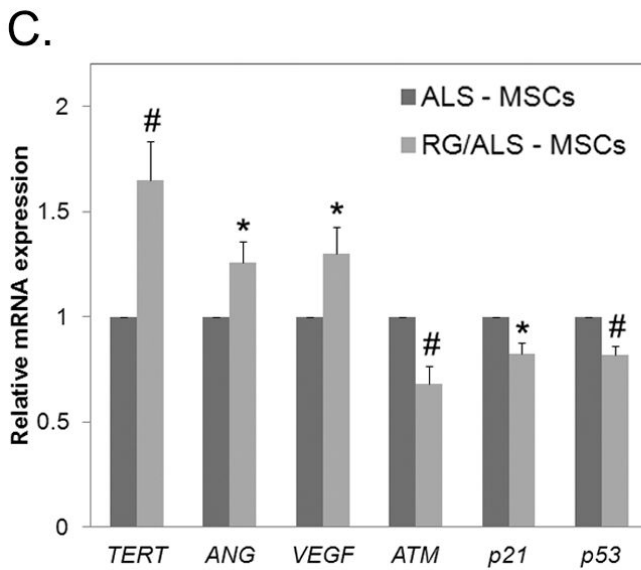
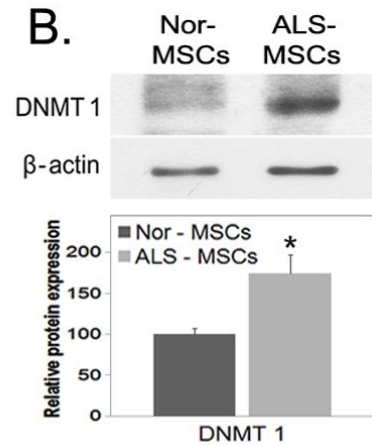
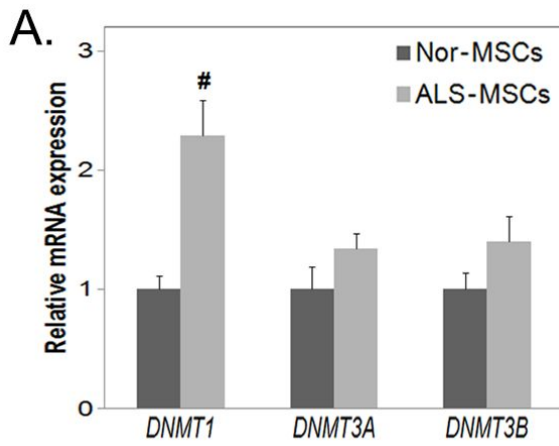


Figure 1. RG108 induces the expression of anti-senescence factors in ALS-MSCs.

(A) The expression levels of DNA methyltransferases *DNMT1*, *DNMT3A*, and *-3B* were examined by real-time PCR in normal hBM-MSCs (Nor-MSCs) and BM-MSCs from ALS patients (ALS-MSCs). (B) The expression of DNMT1 protein were confirmed by immunoblot analysis. Protein expression data were quantified using the Image J software. (C) The expression of the anti-senescence genes *TERT*, *ANG*, *VEGF*, and senescence genes *ATM*, *p21*, *p53* was measured by real-time PCR for RG108-treated ALS-MSCs (RG/ALS-MSCs) and untreated ALS-MSCs. (D) Expression was confirmed by immunoblot analysis with antibodies specific to TERT, p53, or β -actin. Protein expression data were quantified using the Image J software.

III-2. RG108 treatment of ALS-MSCs prevents cellular senescence

I have shown that the expression of anti-senescence factors is altered with RG108 treatment in ALS-MSCs. To further examine this effect, SA- β -gal assays were performed with RG108-treated (0 or 5 μ M, 48 h) ALS-MSCs. The number of SA- β -gal positive cells decreased in RG/ALS-MSCs than in ALS-MSCs (Fig. 2A; *t*-test, #*p*<0.01, mean \pm SD, n=4). The senescence marker proteins were decreased by 84% (p53) and 83% (p16) in RG/ALS-MSCs compared to non-treated ALS-MSCs (Fig. 2B; *t*-test, **p*<0.05, #*p* < 0.01, mean \pm SD, n=4).

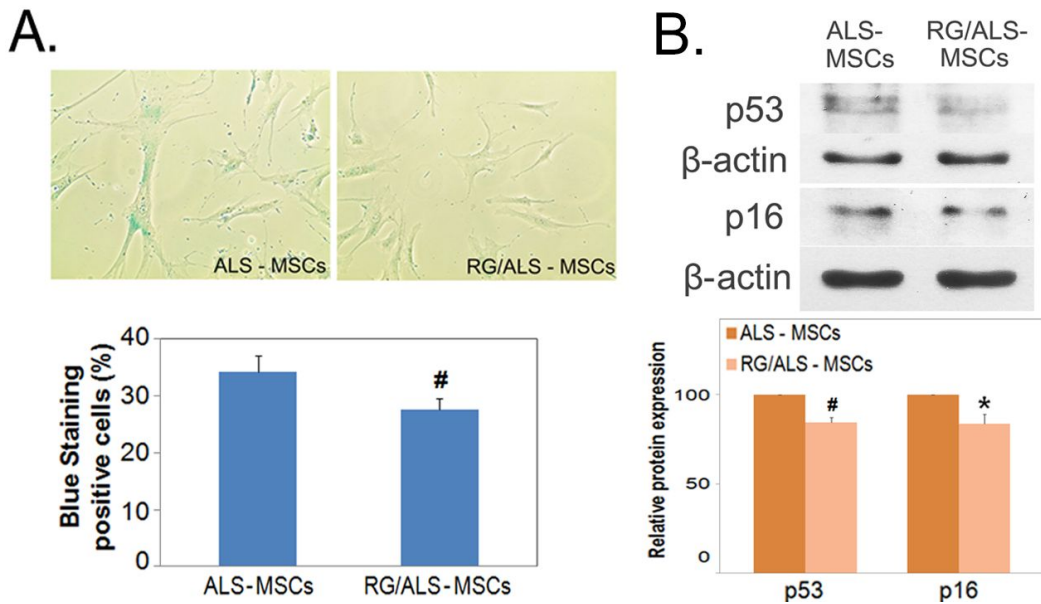


Figure 2. RG108 treatment prevents cellular senescence in ALS-MSCs.

(A) SA- β -gal assays were performed on RG108-treated ALS-MSCs. Senescent cells are indicated by blue staining. The number of total cells and senescent cells (blue color) were counted. (B) The expression of the senescence marker proteins p53 and p16 were confirmed by immunoblot analysis. Protein expression data were quantified using the Image J software.

III-3. Migration and protection potency are improved in RG/ALS-MSCs

ALS-MSCs were incubated with 0 or 5 μ M RG108 for 48 h; cells were examined with a wound healing assay and a cell viability assay. Cell migration rate was increased in RG/ALS-MSCs (Fig. 3A; *t*-test, * p <0.05, mean \pm SD, n =4). For the cell viability assay, RG/ALS-MSCs were exposed to H₂O₂ (0~1.5 mM) for 1.5 h and then subjected to an MTT assay. The viability of RG/ALS-MSCs was significantly increased compared to non-treated ALS-MSCs (Fig. 3B; *t*-test, * p <0.05, # p <0.01, mean \pm SD, n =4).

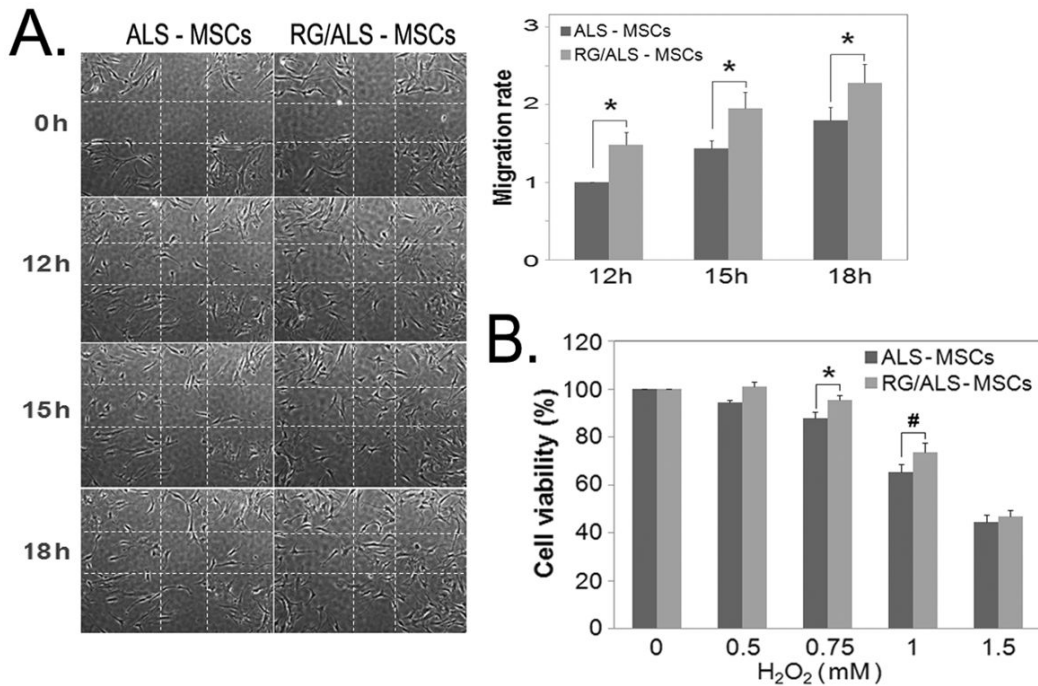


Figure 3. Migration and protective effects were improved in RG108-treated ALS-MSCs.

(A) The migration of RG/ALS-MSCs was observed for 18 h after being scratched (inside dotted line). Migrated cells inside the dotted lines were counted. (B) RG/ALS-MSCs were exposed to 0–1.5 mM H₂O₂ and cell viability was examined by MTT assay.

III-4. RG/ALS-MSCs effectively differentiate into neuron-like cells

Since RG108 significantly induces anti-senescence effects, I examined whether RG/ALS-MSCs would more effectively differentiate into neuronal cells. Both ALS-MSCs and RG/ALS-MSCs were differentiated with neuronal induction medium [37, 51]. Undifferentiated ALS-MSCs exhibited a flattened and spindle-shaped appearance, similar to primary ALS-MSCs, while neuronal differentiated ALS-MSCs (ALS-dMSCs and RG/ALS-dMSCs) exhibited neuronal morphology (Fig. 4A). Cells were considered neuronally differentiated if each cell body had more than two dendrites longer than 60 μm . According to the rate of neuronal differentiation in RG/ALS-dMSCs and ALS-dMSCs, a higher percentage of RG/ALS-dMSCs significantly differentiated into neuron-like cells compared to ALS-dMSCs (Fig. 4B, left panel; t-test, $*p < 0.05$, mean \pm SD, $n=4$). The average neurite number for dMSCs was also significantly greater in RG/ALS-dMSCs (Fig. 4B, middle panel; t-test, $*p < 0.05$; mean \pm SD, $n=4$); however, no significant difference in the average neurite length was observed (Fig. 4B, right panel). To characterize the differentiated cells at the protein level, immunoblot analysis was performed with neuron-specific marker proteins, Nestin and Tuj-1. Both neuronal differentiated ALS-MSCs exhibited increased expression of Nestin (156%) and Tuj-1 (135%) relative to the undifferentiated ALS-MSCs (100%, Fig. 4C). RG108-treated ALS-dMSCs more highly expressed Nestin (132%) and Tuj-1 (140%) than untreated ALS-dMSCs (Fig. 4C), indicating that RG108-treated cells more effectively differentiated into neuron-like cells.

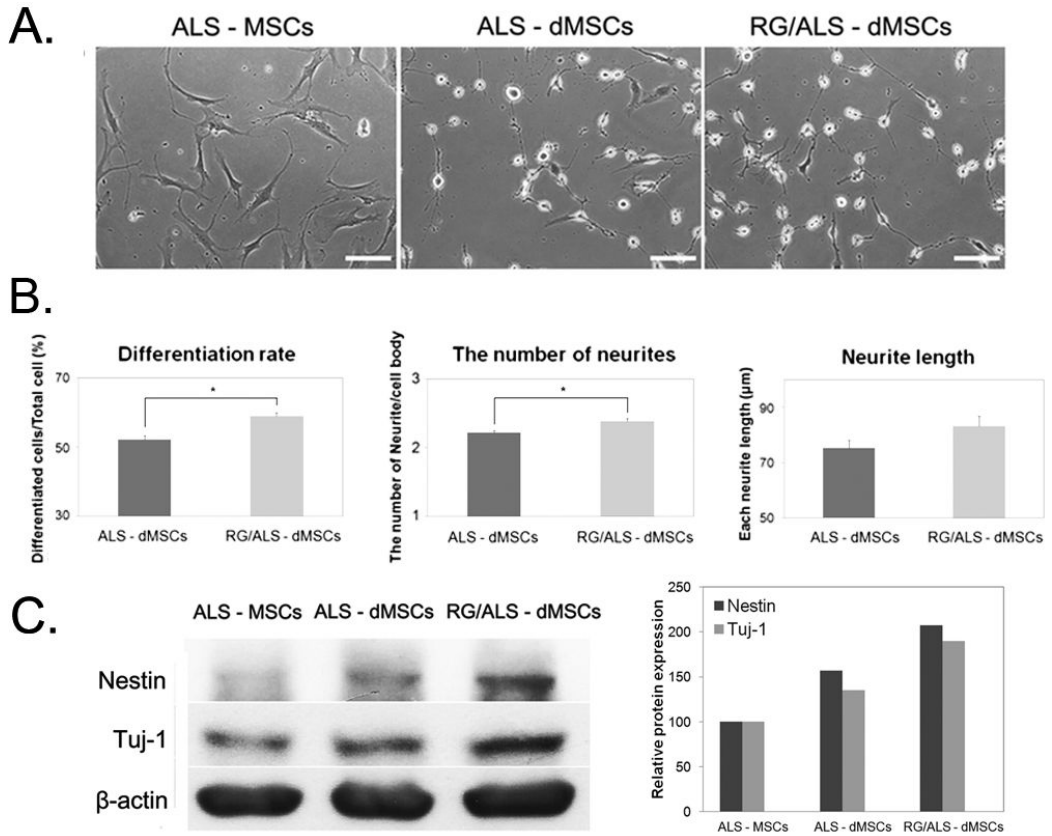


Figure 4. Efficiency of neuronal differentiation was increased in RG108-pre-treated ALS-MSCs.

(A) Both ALS-MSCs and RG/ALS-MSCs were differentiated into neuronal cells following exposure to neuronal induction medium. Neuronal differentiated cells are indicated in ALS-dMSCs and RG/ALS-dMSCs. Scale bar indicates 100 μ m.

(B) Total cells and neuronal-shaped cells were counted to estimate the neuronal differentiation rate (left panel). The number of neurites was significantly increased in RG/ALS-dMSCs (middle panel). No significant difference was observed in neurite length of differentiated cells (right panel).

(C) The differentiated ALS-MSCs were subjected to immunoblot analysis with neuron-specific antibodies, Nestin and Tuj-1. β -Actin was used as an internal standard.

PART II-IV. Discussion

ALS is one of the most common neurodegenerative disorders and is associated with selective motor neuron death [32]. Present study reported that BM-MSCs from ALS patients have diminished stem cell capacity due to decreased secretion of numerous trophic/growth factors [7]. Here, I show that the DNA methyltransferases are excessively expressed in ALS-MSCs (Fig. 1A and 1B). This suggests that the moderation of excessive DNMT1 expression in ALS-MSCs may improve the potency of these stem cells. To examine this hypothesis, the DNMT1 inhibitor RG108 was used. Treatment of ALS-MSCs with RG108 up-regulated the expression of *ANG*, *VEGF* and *TERT*, but down-regulated that of senescence genes (Fig. 1C). Expression was confirmed by immunoblot analysis with specific antibodies to TERT and ANG (Fig. 1D).

Because the aberrantly high DNMT1 expression in ALS-MSCs was effectively modulated with a DNMT1 inhibitor and restored the expression of anti-senescence genes, it seems that RG/ALS-MSCs may exhibit an anti-senescence phenotype. As shown by SA- β -gal assays, the number of β -gal positive cells was reduced in RG108-treated ALS-MSCs relative to untreated ALS-MSCs (Fig. 2A). The expression of cellular senescence-associated proteins, p53 and p16, was also significantly decreased in RG108-treated ALS-MSCs (Fig. 2B).

In stem cell therapy, injected cells have been shown to migrate toward the site of injury [53] and secrete a variety of trophic factors to protect from the surrounding damaged cells [1, 7, 25]. Here, I show that RG108 induces the

expression of the migratory markers VEGF and ANG, and anti-senescence factors. This suggests that RG108 treatment may improve migratory and cell-protective abilities. As presented in Figure 3, RG108-treated ALS-MSCs exhibited significantly improved migration and cell protection against oxidative damage (Fig. 3). Thus, RG108 treatment induces anti-senescence phenotypes by modulating the expression of senescence-associated genes.

The neuronal differentiation ability of stem cells plays an important role in stem cell therapy, specifically for neurodegenerative disorders, such as ALS. hBM-MSCs are multipotent, and have the ability to differentiate into neuron-like cells and several other cell types [37-39]. Here, I evaluated the neuronal differentiation capacity of RG108-treated ALS-MSCs (RG/ALS-MSCs). The ALS-MSCs effectively differentiated into neuron-like cells (dMSCs) at a significantly increased differentiation rate and with an increased number of neurites in RG/ALS-dMSCs (Fig. 4A and 4B). These cells exhibited significantly increased expression of the neuron-specific markers, Nestin and Tuj-1 (Fig. 4C). This indicates that RG/ALS-MSCs more effectively differentiated into neuron-like cells than the control (ALS-MSCs) in the presence of neuronal induction medium.

Conclusion

I have investigated the anti-senescence effects of RG108 in hBM-MSCs and confirmed its amelioration of cellular senescence. These RG108 effects were achieved through the expression of anti-senescence related genes (*TERT*, *bFGF*, *VEGF* and *ANG*). Methylation at the *TERT* promoter region was largely decreased in RG108-treated hBM-MSCs. Also, I investigated the anti-senescence effects of DNMT1 inhibition in ALS-MSCs. Expression of DNMT1 was increased in ALS-MSCs. Modulation of excessively-expressed DNMT1 by RG108 partially restored cellular senescence, migration, and cellular protection in ALS-MSCs. In addition, the RG/ALS-MSCs more effectively differentiated into neuron-like cells when incubated with neuronal induction medium. Thus, the RG108 treatment of ALS-MSCs improves their stem cell potency. This suggests that an optimized dose of RG108 may improve stem cell potency and, ameliorates cellular senescence, which may provide better efficacy in stem cell therapy.

References

- [1] Cho, G.W., Koh, S.H., Kim, M.H., Yoo, A.R., Noh, M.Y., Oh,S., and Kim, S.H., The neuroprotective effect of erythropoietin-transduced human mesenchymal stromal cells in an animal model of ischemic stroke. (2010) *Brain Res.* **1353**, 1-13.
- [2] Koh, S.H., Kim, K.S., Choi, M.R., Jung, K.H., Park, K.S., Chai, Y.G., Roh, W., Hwang, S.J., Ko, H.J., Huh, Y.M., Kim, H.T., and Kim, S.H., Implantation of human umbilical cord-derived mesenchymal stem cells as a neuroprotective therapy for ischemic stroke in rats. (2008) *Brain Res.* **1229**, 233-248.
- [3] Donate, L.E., and Blasco, M.A., Telomeres in cancer and ageing. (2011) *Philos. Trans. R. Soc. Lond. B. Biol. Sci.* **366**, 76-84.
- [4] Flores, I., Canela, A., Vera, E., Tejera, A., Cotsarelis, G., and Blasco, M.A., The longest telomeres: a general signature of adult stem cell compartments. (2008) *Genes Dev.* **22**, 654-667.
- [5] Rossi, D.J., Bryder, D., Seita, J., Nussenzweig, A., Hoeijmakers, J., and Weissman, I.L., Deficiencies in DNA damage repair limit the function of haematopoietic stem cells with age. (2007) *Nature* **447**, 725-729.
- [6] Heeschen, C., Lehmann, R., Honold, J., Assmus, B., Aicher, A., Walter, D.H., Martin, H., Zeiher, A. M., and Dimmeler, S., Profoundly reduced neovascularization capacity of bone marrow mononuclear cells derived from patients with chronic ischemic heart disease. (2004) *Circulation* **109**, 1615-1622.

- [7] Cho, G.W., Noh, M.Y., Kim, H.Y., Koh, S.H., Kim, K.S., and Kim, S. H., Bone marrow-derived stromal cells from amyotrophic lateral sclerosis patients have diminished stem cell capacity. (2010) *Stem Cells Dev.* **19**, 1035-1042.
- [8] Yakushiji, N., Yokoyama, H., and Tamura, K., Repatterning in amphibian limb regeneration: A model for study of genetic and epigenetic control of organ regeneration. (2009) *Semin. Cell Dev. Biol.* **20**, 565-574.
- [9] Palacios, D., and Puri, P.L., The epigenetic network regulating muscle development and regeneration. (2006) *J. Cell. Physiol.* **207**, 1-11.
- [10] Gereige, L.M., and Mikkola, H.K., DNA methylation is a guardian of stem cell self-renewal and multipotency. (2009) *Nat. Genet.* **41**, 1164-1166.
- [11] Weidman, J.R., Dolinoy, D.C., Murphy, S.K., and Jirtle, R.L., Cancer susceptibility: epigenetic manifestation of environmental exposures. (2007) *Cancer J.* **13**, 9-16.
- [12] Jones, P.A., and Baylin, S.B., The epigenomics of cancer. (2007) *Cell* **128**, 683-692.
- [13] Winnefeld, M., and Lyko, F., The aging epigenome: DNA methylation from the cradle to the grave. (2012) *Genome Biol.* **13**, 165.
- [14] Sedivy, J.M., Banumathy, G., and Adams, P.D., Aging by epigenetics--a consequence of chromatin damage? (2008) *Exp. Cell Res.* **314**, 1909-1917.
- [15] Bork, S., Pfister, S., Witt, H., Horn, P., Korn, B., Ho, A.D., and Wagner, W., DNA methylation pattern changes upon long-term culture and aging of human mesenchymal stromal cells. (2010) *Aging Cell.* **9**, 54-63.

- [16] Johnson, A.A., Akman, K., Calimport, S.R., Wuttke, D., Stolzing, A., and de Magalhaes, J.P., The role of DNA methylation in aging, rejuvenation, and age-related disease. (2012) *Rejuvenation Res.* **15**, 483-494.
- [17] So, A.Y., Jung, J.W., Lee, S., Kim, H.S., and Kang, K.S., DNA methyltransferase controls stem cell aging by regulating BMI1 and EZH2 through microRNAs. (2011) *PLoS One* **6**, e19503.
- [18] Kosar, M., Bartkova, J., Hubackova, S., Hodny, Z., Lukas, J., and Bartek, J., Senescence-associated heterochromatin foci are dispensable for cellular senescence, occur in a cell type- and insult-dependent manner and follow expression of p16(ink4a). (2011) *Cell Cycle* **10**, 457-468.
- [19] Choi, M.R., In, Y.H., Park, J., Park, T., Jung, K.H., Chai, J.C., Chung, M.K., Lee, Y.S., and Chai, Y.G., Genome-scale DNA methylation pattern profiling of human bone marrow mesenchymal stem cells in long-term culture. (2012) *Exp. Mol. Med.* **44**, 503-512.
- [20] Okano, M., Bell, D.W., Haber, D.A., and Li, E., DNA methyltransferases Dnmt3a and Dnmt3b are essential for de novo methylation and mammalian development. (1999) *Cell* **99**, 247-257.
- [21] Ahuja, N., and Issa, J.P., Aging, methylation and cancer. (2000) *Histol. Histopathol.* **15**, 835-842.
- [22] Brueckner, B., Garcia Boy, R., Siedlecki, P., Musch, T., Kliem, H.C., Zielenkiewicz, P., Suhai, S., Wiessler, M., and Lyko, F., Epigenetic reactivation of tumor suppressor genes by a novel small-molecule inhibitor of human DNA methyltransferases. (2005) *Cancer Res.* **65**, 6305-6311.
- [23] Siedlecki, P., Garcia Boy, R., Musch, T., Brueckner, B., Suhai, S., Lyko,

- F., and Zielenkiewicz, P., Discovery of two novel, small-molecule inhibitors of DNA methylation. (2006) *J. Med. Chem.* **49**, 678-683.
- [24] Zinn, R.L., Pruitt, K., Eguchi, S., Baylin, S.B., and Herman, J.G., hTERT is expressed in cancer cell lines despite promoter DNA methylation by preservation of unmethylated DNA and active chromatin around the transcription start site. (2007) *Cancer Res.* **67**, 194-201.
- [25] Caplan, A.I., Dennis, J.E., Mesenchymal stem cells as trophic mediators. (2006) *J. Cell Biochem.* **98**, 1076-1084.
- [26] Li, L., and Jiang, J., Regulatory factors of mesenchymal stem cell migration into injured tissues and their signal transduction mechanisms. (2011) *Front Med.* **5**, 33-39.
- [27] d'Adda di Fagagna, F., Living on a break: cellular senescence as a DNA-damage response. (2008) *Nat. Rev. Cancer* **8**, 512-522.
- [28] Harley, C.B., Futcher, A.B., and Greider, C.W., Telomeres shorten during ageing of human fibroblasts. (1990) *Nature* **345**, 458-460.
- [29] Blasco, M.A., Lee, H.W., Hande, M.P., Samper, E., Lansdorp, P.M., DePinho, R.A., and Greider, C.W., Telomere shortening and tumor formation by mouse cells lacking telomerase RNA. (1997) *Cell* **91**, 25-34.
- [30] Lee, H.W., Blasco, M.A., Gottlieb, G.J., Horner, J.W., 2nd, Greider, C.W., and DePinho, R.A., Essential role of mouse telomerase in highly proliferative organs. (1998) *Nature* **392**, 569-574.
- [31] Estrada, J.C., Torres, Y., Benguria, A., Dopazo, A., Roche, E., Carrera-Quintanar, L., Perez, R.A., Enriquez, J.A., Torres, R., Ramirez, J.C., Samper, E., and Bernad, A., Human mesenchymal stem

- cell-replicative senescence and oxidative stress are closely linked to aneuploidy. (2013) *Cell Death Dis.* **4**, e691
- [32] Cleveland, D. W., and Rothstein, J. D., From Charcot to Lou Gehrig: deciphering selective motor neuron death in ALS. (2001) *Nat. Rev. Neurosci.* **2**, 806-819.
- [33] Logroscino, G., Traynor, B. J., Hardiman, O., Chio, A., Couratier, P., Mitchell, J. D., Swingler, R. J., and Beghi, E., Descriptive epidemiology of amyotrophic lateral sclerosis: new evidence and unsolved issues. (2008) *J. Neurol. Neurosurg. Psychiatry* **79**, 6-11.
- [34] Garbuzova-Davis, S., Woods, R. L., 3rd, Louis, M. K., Zesiewicz, T. A., Kuzmin-Nichols, N., Sullivan, K. L., Miller, A. M., Hernandez-Ontiveros, D. G., and Sanberg, P. R., Reduction of circulating endothelial cells in peripheral blood of ALS patients. (2010) *PLoS One* **5**, e10614.
- [35] Xi, Z., Zinman, L., Moreno, D., Schymick, J., Liang, Y., Sato, C., Zheng, Y., Ghani, M., Dib, S., Keith, J., Robertson, J., and Rogaeva, E., Hypermethylation of the CpG island near the G4C2 repeat in ALS with a C9orf72 expansion. (2013) *Am. J. Hum. Genet.* **92**, 981-989.
- [36] Bossolasco, P., Cova, L., Calzarossa, C., Servida, F., Mencacci, N. E., Onida, F., Polli, E., Lambertenghi Delilieri, G., and Silani, V., Metalloproteinase alterations in the bone marrow of ALS patients. (2010) *J. Mol. Med.* **88**, 553-564.
- [37] Jeong, S. G., Ohn, T., Kim, S. H., and Cho, G. W., Valproic acid promotes neuronal differentiation by induction of neuroprogenitors in human bone-marrow mesenchymal stromal cells. (2013) *Neurosci. Lett.*

554, 22-27.

- [38] Caplan, A. I., Adult mesenchymal stem cells for tissue engineering versus regenerative medicine. (2007) *J. Cell. Physiol.* **213**, 341-347.
- [39] Pittenger, M. F., Mackay, A. M., Beck, S. C., Jaiswal, R. K., Douglas, R., Mosca, J. D., Moorman, M. A., Simonetti, D. W., Craig, S., and Marshak, D. R., Multilineage potential of adult human mesenchymal stem cells. (1999) *Science* **284**, 143-147.
- [40] Boido, M., Piras, A., Valsecchi, V., Spigolon, G., Mareschi, K., Ferrero, I., Vizzini, A., Temi, S., Mazzini, L., Fagioli, F., and Vercelli, A., Human mesenchymal stromal cell transplantation modulates neuroinflammatory milieu in a mouse model of amyotrophic lateral sclerosis. (2014) *Cytotherapy* **16**, 1059-1072.
- [41] Kim, H., Kim, H. Y., Choi, M. R., Hwang, S., Nam, K. H., Kim, H. C., Han, J. S., Kim, K. S., Yoon, H. S., and Kim, S. H., Dose-dependent efficacy of ALS-human mesenchymal stem cells transplantation into cisterna magna in SOD1-G93A ALS mice. (2010) *Neurosci. Lett.* **468**, 190-194.
- [42] Li, E., and Zhang, Y., DNA methylation in mammals. (2014) *Cold. Spring. Harb. Perspect. Biol.* **6**, a019133.
- [43] Ammal Kaidery, N., Tarannum, S., and Thomas, B., Epigenetic landscape of Parkinson's disease: emerging role in disease mechanisms and therapeutic modalities. (2013) *Neurotherapeutics* **10**, 698-708.
- [44] De Jager, P. L., Srivastava, G., Lunnon, K., Burgess, J., Schalkwyk, L. C., Yu, L., Eaton, M. L., Keenan, B. T., Ernst, J., McCabe, C., Tang, A.,

- Raj, T., Replogle, J., Brodeur, W., Gabriel, S., Chai, H. S., Younkin, C., Younkin, S. G., Zou, F., Szyf, M., Epstein, C. B., Schneider, J. A., Bernstein, B. E., Meissner, A., Ertekin-Taner, N., Chibnik, L. B., Kellis, M., Mill, J., and Bennett, D. A., Alzheimer's disease: early alterations in brain DNA methylation at ANK1, BIN1, RHBDF2 and other loci. (2014) *Nat. Neurosci.* **17**, 1156-1163.
- [45] Alvarez, K., de Andres, M. C., Takahashi, A., and Oreffo, R. O., Effects of hypoxia on anabolic and catabolic gene expression and DNA methylation in OA chondrocytes. (2014) *BMC Musculoskelet. Disord.* **15**, 431.
- [46] Hoile, S. P., Clarke-Harris, R., Huang, R. C., Calder, P. C., Mori, T. A., Beilin, L. J., Lillycrop, K. A., and Burdge, G. C., Supplementation with N-3 long-chain polyunsaturated fatty acids or olive oil in men and women with renal disease induces differential changes in the DNA methylation of FADS2 and ELOVL5 in peripheral blood mononuclear cells. (2014) *PLoS One* **9**, e109896.
- [47] Chestnut, B. A., Chang, Q., Price, A., Lesuisse, C., Wong, M., and Martin, L. J., Epigenetic regulation of motor neuron cell death through DNA methylation. (2011) *J. Neurosci.* **31**, 16619-16636.
- [48] Tremolizzo, L., Messina, P., Conti, E., Sala, G., Cecchi, M., Airoidi, L., Pastorelli, R., Pupillo, E., Bandettini Di Poggio, M., Filosto, M., Lunetta, C., Agliardi, C., Guerini, F., Mandrioli, J., Calvo, A., Beghi, E., and Ferrarese, C., Whole-blood global DNA methylation is increased in amyotrophic lateral sclerosis independently of age of onset. (2014)

- Amyotroph. Lateral Scler. Frontotemporal Degener.* **15**, 98-105.
- [49] Schirmacher, E., Beck, C., Brueckner, B., Schmitges, F., Siedlecki, P., Bartenstein, P., Lyko, F., and Schirmacher, R., Synthesis and in vitro evaluation of biotinylated RG108: a high affinity compound for studying binding interactions with human DNA methyltransferases. (2006) *Bioconjug. Chem.* **17**, 261-266.
- [50] Kim, H. Y., Kim, H., Oh, K. W., Oh, S. I., Koh, S. H., Baik, W., Noh, M. Y., Kim, K. S., and Kim, S. H., Biological markers of mesenchymal stromal cells as predictors of response to autologous stem cell transplantation in patients with amyotrophic lateral sclerosis: an investigator-initiated trial and in vivo study. (2014) *Stem Cells* **32**, 2724-2731.
- [51] Joe, I. S., Jeong, S. G., and Cho, G. W., Resveratrol-induced SIRT1 activation promotes neuronal differentiation of human bone marrow mesenchymal stem cells. (2015) *Neurosci. Lett.* **584**, 97-102.
- [52] Belzil, V. V., Bauer, P. O., Gendron, T. F., Murray, M. E., Dickson, D., and Petrucelli, L., Characterization of DNA hypermethylation in the cerebellum of c9FTD/ALS patients. (2014) *Brain Res.* **1584**, 15-21.
- [53] Sohni, A., and Verfaillie, C. M., Mesenchymal stem cells migration homing and tracking. (2013) *Stem Cells Int.* **2013**, 130763.